Accepted Manuscript

Complex refractive index of InXGa1-XN thin films grown on cubic (100) GaN/MgO

H. Vilchis, V.D. Compeán-García, I.E. Orozco-Hinostroza, E. López-Luna, M.A. Vidal, A.G. Rodríguez

Please cite this article as: H. Vilchis, V.D. Compeán-García, I.E. Orozco-Hinostroza, E. López-Luna, M.A. Vidal, A.G. Rodríguez , Complex refractive index of InXGa1-XN thin films grown on cubic (100) GaN/MgO. The address for the corresponding author was captured as affiliation for all authors. Please check if appropriate. Tsf(2016), doi: 10.1016/j.tsf.2017.02.016

Complex refractive index of $In_XGa_{1-X}N$ thin films grown on cubic (100) GaN/MgO

H. Vilchis[a], V. D. Compeán-García[b], I. E. Orozco-Hinostroza[c], E. López-Luna[a], M. A. Vidal[a], A. G. Rodríguez[a,*]

a) Coordinación para la Innovación y la Aplicación de la Ciencia y la Tecnología (CIACYT), Universidad Autónoma de San Luis Potosí, Álvaro Obregón 64, 78000 San Luis Potosí, S.L.P., México
b) CONACYT - Universidad Autónoma de San Luis Potosí, Álvaro Obregón 64, 78000 San Luis Potosí, S.L.P., México
c) Instituto Potosino de Investigación Científica y Tecnológica (IPICYT), Camino a la Presa San José 2055, Col. Lomas 4a Sección, 78216 San Luis Potosí, S.L.P., México

ABSTRACT

Spectroscopic ellipsometry measurements of $In_XGa_{1-X}N$ thin films were carried out in the photon energy range from 0.6 to 4.75 eV. The samples were grown on cubic GaN/MgO (100) template substrates by plasma assisted molecular beam epitaxy. Optical properties as the energy gap, refractive index (η) and extinction coefficient (κ) were obtained from the analysis of experimental data by a parametric dielectric function model. Our results show that the behavior of the optical band gap of cubic $In_XGa_{1-X}N$ fits $E_g(x) = 1.407x^2 - 3.662x + 3.2$ eV. The obtained bowing parameter of 1.4 ± 0.1 eV is in good agreement with reported calculated values around 1.37 eV. The complex index of refraction dispersion relations $\eta(\omega)$ and $\kappa(\omega)$ are obtained for the 85 – 99% mostly cubic $In_XGa_{1-X}N$ films for several In concentrations.

*Corresponding author: angel.rodriguez@uaslp.mx

1

1. Introduction

During the last decade, $In_XGa_{1-X}N$ and $In_XGa_{1-X}N$/III-N heterostructures have attracted considerable attention due to their great potential in technological applications. Their properties such as peak electron velocity, absorption edge, and high thermal stability have been exploited for the manufacture of electronics, photonics and nanotechnology devices. [1-3] Furthermore, the $In_XGa_{1-X}N$ alloy system has the singular possibility of tuning its band gap energy from near UV to IR only by varying the In molar fraction. [4,5] Hence, $In_XGa_{1-X}N$ is specifically suitable in blue-green-red emitting devices, as well as photodetectors, laser and solar cell devices. [6-9]

On the other hand, for the technological development of the above devices, it is key the study of vertical transport using basically the double-barrier (DB) formed by thin films. In these structures with stable hexagonal phase (h-$In_XGa_{1-X}N$ alloys), spontaneous and piezoelectric polarizations induce electric fields in the structure that are perpendicular to the growth direction, resulting in tilted energy bands. [10] These built-in fields are undesirable because they decrease the lifetime operation in optical devices. The growth of the meta-stable cubic phase of III-N and $In_XGa_{1-X}N$ alloys (c-$In_XGa_{1-X}N$) is a possibility to avoid these built-in fields, because the cubic crystal symmetry avoids spontaneous polarizations. [11] In addition, it is expected that cubic nitrides have superior electronic properties such as higher carrier mobilities, higher drift velocities, and better doping efficiencies. [12, 13] So, several research groups have grown c-$In_XGa_{1-X}N$ films [1, 14-21] with different x concentrations. Recently, homogenous c-$In_XGa_{1-X}N$ films with x up to 0.93 have been reported. [18]

In the development of semiconductor devices for technological applications, as those mentioned above, the knowledge of key fundamental properties is essential for

the design, modeling and understanding of the devices performance. So it is necessary to know the fundamental electrical and optical properties; in the case of c-$In_XGa_{1-X}N$ alloys their electrical properties have been extensively studied, however, optical properties have been barely investigated.

The refractive index for c-$In_XGa_{1-X}N$ was reported by Goldhan et al. in 2000, [14] their results showed the refractive index and the extinction coefficient in the range from 1 to 4 eV for relaxed films only for films with In concentration less than 0.2. Although different groups have contributed to the study of the optical properties of c-$In_XGa_{1-X}N$ [15, 22, 23], it has not been possible to define their characteristics for In concentrations greater than 0.4 due to the difficulty to obtain homogenous alloys [24]. The dielectric function of GaN, $In_XGa_{1-X}N$, $Al_xGa_{1-x}N$ and $Al_{1-x}In_xN$ has been mainly reported for hexagonal phase films and the optical parameters reports of cubic nitride alloys are still scarce. [25-29]

Therefore, the objective of this work is to determine the dispersion relations for the complex refraction index in the photon energy range from 0.6 to 4.75 eV of mostly cubic $In_XGa_{1-X}N$ films grown on cubic GaN/MgO template substrates for several In molar fractions up to x = 1. The complex refractive index, optical energy gap and crystalline quality of $In_XGa_{1-X}N$ were obtained from the experimental data using a multilayer parametric model for the dielectric function.

2. Experimental procedure

We used (100) MgO as growth substrates. Prior to each growth a 1x1 cm polished MgO substrate was cleaned in trichloroethylene at 60 °C and acetone ultrasonic bath for 10 min. After that, the substrate was introduced into a vacuum loading chamber and was then transferred to the growth chamber and thermally cleaned in a high vacuum

3

environment (3 x 10^{-8}Torr) at Ts = 900 °C for 30 min to obtain a clean and atomically flat surface. Before growing the In$_X$Ga$_{1-X}$N film, a cubic GaN buffer layer was grown on the MgO substrate, experiment details of this film can be found elsewhere. [18]

The cubic GaN/MgO templates are essential to induce the growth of cubic In$_X$Ga$_{1-X}$N films. [18] InGaN layers were grown at a substrate temperature between 560 and 650 °C on top of a c-GaN/MgO (100) template substrate. The alloy composition was obtained from the lattice parameter measured by high resolution X-ray diffraction and the fraction of the cubic phase was estimated from the ratio of integrated intensities of the (111) zinc blend diffraction at χ=54.74° and (0002) wurzite reflections at χ=0° in XRD pole figures. [18] For samples with low and high In concentration the cubic phase fraction was up to 99%, but In$_X$Ga$_{1-X}$N layers with 0.3 < x < 0.8 show hexagonal inclusions fractions around 15%. [18]

The optical properties of the samples were measured ex-situ at room temperature by spectroscopic ellipsometry from 0.60 to 4.75 eV using a Horiba-Uvisel ellipsometer in the modulator (M) and analyzer (A) configurations M = 0°, A = +45° and M = - 45° and A = +45° with an incidence angle of 70°. This ellipsometer is a phase-modulation instrument (PME) where fast and accurate measurements from the UV to the near infrared region can be performed. The spectroscopic angles Ψ and Δ are not directly measured by PME, instead the Fourier coefficients $I_S = Sin2\Psi Cos\Delta$ and $I_C = Sin2\Psi Sin\Delta$ are obtained. Under these conditions and using an integration time of 500 ms for each data point the expected experimental error in Ψ and Δ are 0.03% and 0.02% respectively. The analyses of the samples were carried out fitting these Is, Ic directly. [30]

3. Results and discussions

4

The experimental ellipsometric spectra of cubic GaN/MgO template is shown in Fig. 1 (a) as solid squares (circles) for Is (Ic). Interference fringes due to the GaN layer thickness are clearly observed in the semitransparent region below the GaN optical gap. As a buffer layer with similar growth conditions was later used for the growth of each $In_XGa_{1-X}N$ layer the optical parameters of the template were needed to minimize the number of fitting parameters of the studied samples. Both the c-GaN/MgO template and $In_XGa_{1-X}N$ /c-GaN/MgO heterostructures were modeled considering a single oscillator dispersion for each GaN and $In_XGa_{1-X}N$ layer (j) with real (η) and imaginary (κ) parts of the complex refractive index given by

$$\eta(\omega) = \eta_\infty + \frac{B(\omega - \omega_j) + C}{(\omega - \omega_j)^2 + \Gamma_j^2} \tag{1}$$

$$\kappa(\omega) = \begin{cases} 0 \quad, & \omega \leq \omega_g \\ \frac{f_j(\omega - \omega_g)^2}{(\omega - \omega_j)^2 + \Gamma_j^2}, & \omega > \omega_g \end{cases} \tag{2}$$

where

$$B = \frac{f_j}{\Gamma_j}\left(\Gamma_j^2 - (\omega_j - \omega_g)^2\right) \tag{3}$$

$$C = 2f_j\Gamma_j(\omega_j - \omega_g) \tag{4}$$

And η_∞ is the high frequency refractive index, Γ_j is the optical broadening, f_j the oscillator strength, ω_j the oscillator frequency and ω_g the optical gap frequency. [31]

Solid lines in Fig. 1 (a) show the modeled ellipsometric spectra for the c-GaN/MgO template using the optical parameters given in Table 1. These parameters, except for the c-GaN layer thickness, will be fixed during the modeling of the $In_XGa_{1-X}N$/c-GaN/MgO heterostructures. The complex dielectric function of c-GaN obtained from the model is shown in Fig. 1 (b) which is in very good agreement with the reported dielectric function of c-GaN. [25], evidencing that the fitting model is appropriate for the studied photon energy interval. A more detailed model for the dielectric function is

5

needed for wider energy intervals. [26, 27] We have to note that previous to the modeling of the template substrates and the samples, the optical parameters of the MgO substrates were also measured in order to reduce the fitting parameters of the heterostructures.

The ellipsometric spectra of the $In_XGa_{1-X}N$/c-GaN/MgO samples are plotted in Fig. 2 for different x concentrations. Interference fringes due to the layers thickness are present for all samples. It is clear the shift to lower energy of the onset of the semitransparent region as the optical gap of $In_XGa_{1-X}N$ decreases with x concentration. The spectra of each sample were fitted using the model above adding the corresponding $In_XGa_{1-X}N$ layer. As obtained from the fit, the optical parameters of each film are given in Table 1. Surface roughness was included in the model considering effective medium theory with a top layer of 50% air and 50% $In_XGa_{1-X}N$. [30] The obtained roughness show relatively good agreement with the root mean square roughness determined by atomic force microscopy (AFM). The values are not exactly the same because ellipsometry results include the effect of a larger area which cannot be detected by AFM. [30] The values of the optical gap decrease as expected with x concentration, these values obtained from the fit may seem lower than those apparent from the plots of Fig. 2. However, the interference fringe onsets in the graph are a combined effect of the heterostructure since the c-GaN buffer layer is thicker than the $In_XGa_{1-X}N$ films in order to optimize the structural quality of the alloy. [18]

The optical gap values from Table 1 are compared to previously reported data of cubic $In_XGa_{1-X}N$ in Fig. 3 (solid squares). The values reported by Pacheco-Salazar [15] *et al* and Sun *et al* [22] were both obtained from photoluminescence spectra and those of Ref. 18 were obtained from the optical transmission. The observed differences may be due to the fact that the values reported in this work were extracted from the model

for the $In_XGa_{1-X}N$ layer only and not from the whole heterostructure of the sample. The solid line is a minimum square fit to the ellipsometry data, keeping fixed the intercept (x=0) at 3.2 eV, given by $E_g(x) = 1.407x^2 - 3.662x + 3.2$ eV. The obtained value for the bowing parameter b = 1.4 ± 0.1 eV is in very good agreement with the reported calculated values of 1.36, 1.37 and 1.379. [32-34]

There is a lack of experimental values of the optical gap for 0.5 < x < 0.9, due to homogenous $In_XGa_{1-X}N$ alloys have not yet been experimentally obtained in this concentration interval where phase separation precludes a homogenous growth. In fact, reports of cubic $In_XGa_{1-X}N$ for x > 0.3 are scarce. [18] The plot of the optical broadening (Γ) obtained from the model for the $In_XGa_{1-X}N$ alloys as a function of the x concentration is shown in Fig. 4. The values in Table 1 were normalized to the optical broadening of GaN ($\Gamma_{InGaN}/\Gamma_{GaN}$), this ratio should be higher for alloys of lower crystalline quality compared to the GaN buffer layer. It can be seen that the quality worsens in relation to GaN as the x concentration is increased, reaching a maximum in the interval boundaries where no homogenous alloys can be grown, the solid line in the graph is for visual aid only, showing the deterioration of the quality with x concentration. In contrast, around x = 0 and x =1 the layers have a better crystalline quality than the GaN buffer layer.

Finally, the complex refraction indexes for $In_XGa_{1-X}N$ as obtained from the model are shown in Fig 5. The plots for other x concentrations can be obtained from equations (1) to (4) and the parameters in Table 1. The values and line shapes of the index of refraction and extinction coefficient are similar to those reported for hexagonal $In_XGa_{1-X}N$, [26] which are also scarce in the literature as a function of the In molar fraction. From Ref. 26, the refractive index in the semitransparent region (η_S) and the extinction

7

coefficient above the optical gap (κ_o) of h-In$_X$Ga$_{1-X}$N at x = 0.15 are η_S = 2.4 and κ_o = 0.3. Meanwhile, for our In$_X$Ga$_{1-X}$N films, we obtained at x = 0.10 and x = 0.12 the following values η_S = 2.15, κ_o = 0.28 and η_S = 2.13, κ_o = 0.5 respectively. These values are comparable to those of the hexagonal phase, but η_S is smaller in the cubic films. The extinction coefficient is zero below the energy band gap and the onset where it begins to increase is as expected E$_g$(x). Thus, we report the complex index of refraction that is obtained from spectroscopic ellipsometry of mostly cubic In$_X$Ga$_{1-X}$N films for several In molar concentrations. These dispersion relations should be of great interest to aid the design of optoelectronic devices based on cubic nitride alloys.

4. Conclusion

We determined the complex index of refraction dispersion relations of 85 – 99% cubic phase In$_X$Ga$_{1-X}$N films using spectroscopic ellipsometry in the photon energy range from 0.6 to 4.75 eV. These optical parameters, obtained from cubic material, exhibit similar line shapes to those of hexagonal III-nitride alloys. The behavior of the optical energy gap is fitted to a parabolic curve with a bowing parameter of 1.4 ± 0.1 eV, which is in good agreement with calculated values reported in the literature of 1.37 eV. The optical broadening obtained from the model shows the behavior of the In$_X$Ga$_{1-X}$N crystalline quality with x concentration, with a clear deterioration close to the 0.5 < x < 0.9 intervals where no homogenous alloys have been grown.

Acknowledgments

8

References

[1] N. Yahyaoui, N. Sfina, S. Abdi-Ben Nasrallah, J.-L. Lazzari, M. Said, Electron transport through cubic InGaN/AlGaN resonant tunneling diodes, *Computer Physics Communications* **185** (2014) 3119.

[2] E. Nakamura, K. Ueno, J. Ohta, H. Fujioka, M. Oshima, Dramatic reduction in process temperature of InGaN-based light-emitting diodes by pulsed sputtering growth technique, *Appl. Phys. Lett.* **104** (2014) 051121.

[3] A. Yamamoto, K. Kodama, Md. Tanvir, N. Shigekawa, and Masaaki Kuzuhara, MOVPE growth of thick (>1 µm) InGaN on AlN/Si substrates for InGaN/Si tandem solar cells, *Jpn. J. Appl. Phys.* **54** (2015) 08KA12.

[4] S. Nakamura, M. Senoh, N. Iwasa, S. Nagahama, T. Yamada, and T. Mukai, Superbright Green InGaN Single-Quantum-Well-Structure Light-Emitting Diodes, *Jpn. J. Appl. Phys.* **34** (1995) L1332.

[5] S. Hernández, R. Cuscó, D. Pastor, L Artús, K.P. O'Donell, R.W. Martin, I.M. Watson, Y. Nanishi, E. Calleja, Raman-scattering study of the InGaN alloy over the whole composition range, *J. Appl. Phys.* **98** (2005) 013511.

[6] J. Zhang, and N. Tansu, Improvement in spontaneous emission rates for InGaN quantum wells on ternary InGaN substrate for light-emitting diodes, *J. Appl. Phys.* **110** (2011) 113110.

[7] J. Zhang, and N. Tansu, Optical Gain and Laser Characteristics of InGaN Quantum Wells on Ternary InGaN Substrates, IEEE Photonics Journal **5** (2013) 2600111.

[8] C. J. Neufeld, N. G. Toledo, S. C. Cruz, M. Iza, S. P. DenBaars, and U. K. Mishra, High quantum efficiency InGaN/GaN solar cells with 2.95 eV band gap, *Appl. Phys. Lett.* **93** (2008) 143502.

[9] E. Matioli, C. Neufeld, M. Iza, S. C. Cruz, A. A. Al-Heji, X. Chen, R. M. Farrell, S. Keller, S. DenBaars, U. Mishra, S. Nakamura, J. Speck, and C. Weisbuch, High internal and external quantum efficiency InGaN/GaN solar cells, *Appl. Phys. Lett.* **98 (2011)** 021102.

[10] S. Chichibu, T. Azuhata, T. Sota, S. Nakamura, Spontaneous emission of localized excitons in InGaN single and multiquantum well structures, *Appl. Phys. Lett.* **69** (1996) 4188.

[11] D.J. As, Cubic group-III nitride-based nanostructures-basics and applications in optoelectronics, *Microelectron. J.* **40** (2009) 204.

[12] O. Ambacher, J. Majewski, C. Miskys, A. Link, M.Hermann, M. Eickhoff, M. Stutzmann, F. Bernardini, V. Fiorentini, V. Tilak, B. Schaff, L.F. Eastman, Pyroelectric properties of Al(In)GaN/GaN hetero- and quantum well structures, *J. Phys.: Condens. Matter* **14** (2002) 3399.

[13] C. Mietze, M. Landmann, E. Rauls, H. Machhadani, S. Sakr, M. Tchernycheva, F. H. Julien, W. G. Schmidt, K. Lischka, and D. J. As, Band offsets in cubic GaN/AlN superlattices, *Phys. Rev. B* **83** (2011)195301.

[14] R. Goldhahn, J. Scheiner, S. Shokhovets, T. Frey, U. Kohler, D.J. As, K. Lischka, Refractive index and gap energy of cubic $In_XGa_{1-X}N$, *Appl. Phys. Lett.* **76 (2000)** 291.

[15] D.G. Pacheco-Salazar,J.R. Leite,F. Cerdeira, E.A. Meneses, S.F. Li, D.J. As, K. Lischka, Photoluminescence measurements on cubic InGaN layers deposited on a SiC Substrate, *Semicond. Sci. Technol.* **21** (2006) 846.

[16] S.F. Chichibu, M. Sugiyama, T. Kuroda, A. Tackeuchi, T. Kitamura, H. Nakanishi, T.Sota, S.P. Den Baars, S.Nakamura,Y. Ishida, H. Okumura, Band gap bowing and exciton localization in strained cubic InXGa1−XN films grown on 3C-SiC (001) by rf molecular-beam epitaxy, *Appl. Phys. Lett.* **79 (2001)** 3600

[17] S. Berrah, A. Boukortt, H. Abid, Optical properties of the cubic alloy (In,Ga)N, *Physica E* **41** (2008) 701.

[18] V.D. Compeán-García, I.E. Orozco Hinostroza, A. Escobosa Echavarría, E. López-Luna, A.G. Rodríguez, M.A. Vidal, Bulk lattice parameter and band gap of cubic InXGa1-XN (001) alloys on MgO (100) substrates, *J.Crys. Growth* **418** (2015) 120.

[19] R. Liu and C. Bayram, Maximizing cubic phase gallium nitride surface coverage on nano-patterned silicon (100), Appl. Phys. Lett. **109** (2016) 042103.

[20] I.E. Orozco Hinostroza, M. Avalos-Borja, V.D. Compeán-García, C. Cuellar Zamora, A.G. Rodríguez, E. López-Luna, M.A. Vidal, Tuning emission in violet, blue, green and red in cubic GaN/InGaN/GaN quantum wells, J.Crys. Growth **435** (2016) 110.

[21] C. Bayram, J. A. Ott, K.-T Shiu, C.W. Cheng, Y. Zhu, J. Kim, M. Razeghi, and D. K. Sadana, Gallium Nitride: Cubic Phase GaN on Nano-grooved Si (100) via Maskless Selective Area Epitaxy, Adv. Funct. Mater. **24** (2014) 4491.

[22] X.L. Sun, Y.T. Wang, L.X. Hui Yang, D.P. Zheng, J.B. Xu, Li, Z.G. Wang, Strain and photoluminescence characterization of cubic (In,Ga)N films grown on GaAs(001) substrates, *J. Appl. Phys.* **87** (2000) 3711.

[23] J. Schörmann, D.J.As, K.Lischka, P.Schley, R.Goldhahn, S.F.Li, W.Löffler, M.Hetterich, H.Kalt, Molecular beam epitaxy of phase pure cubic InN, *Appl. Phys. Lett.* **89** (2006) 261903.

11

[24] V.D. Compeán-García, I.E. Orozco-Hinostroza, A. Escobosa-Echavarria, E. López-Luna, A.G. Rodriguez, M.A. Vidal, High-quality InN films on MgO (100) substrates: The key role of 30° in-plane rotation, *Appl. Phys. Lett.* **104** (2014) 191904.

[25] M. Feneberg, M. Röppischer, C. Cobet, N. Esser, J. Schörmann, T. Schupp, D. J. As, F. Hörich, J. Bläsing, A. Krost, R. Goldhahn, Optical properties of cubic GaN from 1 to 20 eV, *Phys. Rev. B* **85** (2012) 155207.

[26] E. Sakalauskas, Ö. Tuna, A. Kraus, H. Bremers, U. Rossow, C. Giesen, M. Heuken, A. Hangleiter, G. Gobsch, R. Goldhahn, Dielectric function and bowing parameters of InGaN alloys, *Phys. Status Solidi b* **249 (**2012**)** 485.

[27] E. Sakalauskas, H. Behmenburg, C. Hums, P. Schley, G. Rossbach, C. Giesen, M. Heuken, H. Kalisch, R. H. Jansen, J. Bläsing, A. Dadgar, A. Krost, R. Goldhahn, Dielectric function and optical properties of Al-rich AlInN alloys pseudomorphically grown on GaN, *J. Phys. D: Appl. Phys.* **43** (2010) 365102.

[28] S. Alajlouni, Z. Y. Sun, J. Li, J. M. Zavada, J.Y. Lin, H.X. Jiang, Refractive index of erbium doped GaN thin films, *Appl. Phys. Lett.* **105** (2014) 081104

[29] K. Kojima, D. Kagaya, Y. Yamazaki, H. Ikeda, K. Fujito, S. F. Chichibu, Spectroscopic ellipsometry studies on the m-plane $Al_{1-x}In_xN$ epilayers grown by metalorganic vapor phase epitaxy on a freestanding GaN substrate, *Japanese J. Appl. Phys.* **55** (2016) 05FG04

[30] H. Fujiwara, *Spectroscopic Ellipsometry Principles and Applications*, Wiley, 2007.

[31] P. Yu and M. Cardona, *Fundamentals of Semiconductors: Physics and Material Properties*, Springer, 1999.

[32] S. Berrah, H. Abid, A. Boukortt, Cohesive properties and energy band-gap of cubic $Al_xGa_yIn_{1-x-y}N$ quaternary alloys, *Phys. Scr.* **74** (2006) 104.

ACCEPTED MANUSCRIPT

[33] M. Marques, L.K. Teles, L.M.R. Scolfaro, J. R. Leite, Lattice parameter and energy band gap of cubic AlxGayIn1−x−yNAlxGayIn1−x−yN quaternary alloys, *Appl. Phys. Lett.* **83 (**2003**)** 890.

[34] W.W. Lin, Y. K. Kuo, B.T. Liou,. Band-Gap Bowing Parameters of the Zincblende Ternary III–Nitrides Derived from Theoretical Simulation, Jpn. *J. Appl. Phys.* **43** (2004) 113.

Figure captions

Fig 1. (a) Ellipsometric spectra of cubic GaN buffer layer on (100) MgO, (b) GaN real and imaginary dielectric function obtained from the analysis of the spectra.

Fig 2. Ellipsometric spectra of $In_XGa_{1-X}N$/c-GaN/MgO samples for several x concentrations. The data of Is and Ic are given in solid squares and open circles respectively.

Fig. 3. Solid squares give the optical band gap of cubic $In_XGa_{1-X}N$ obtained from the model of the dielectric function. The solid line is a quadratic fit with a bowing parameter of 1.4 ± 0.1 eV.

Fig. 4. Optical broadening of $In_XGa_{1-X}N$ normalized to the broadening of GaN. The crystalline quality of the grown films worsens in relation to GaN as the x concentration is closer to the interval $0.5 < x < 0.9$ where no homogenous alloys have been grown.

Fig 5. Refractive index and extinction coefficient dispersion curves of cubic $In_XGa_{1-X}N$, obtained from the analysis of the experimental ellipsometric spectra.
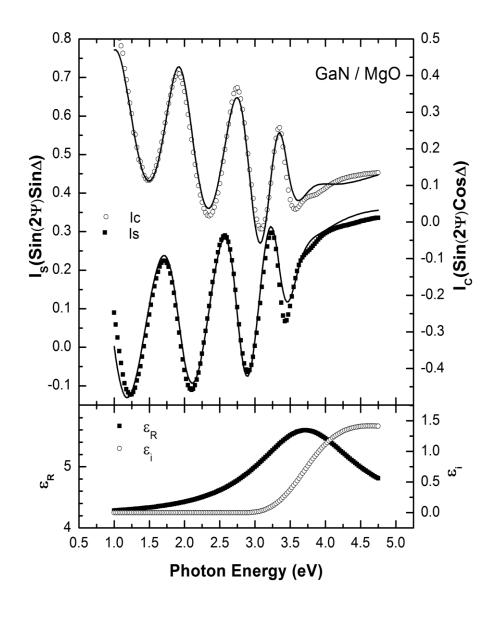
Table captions

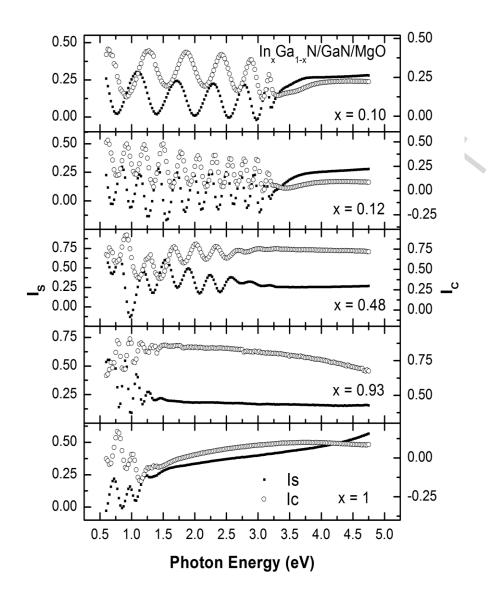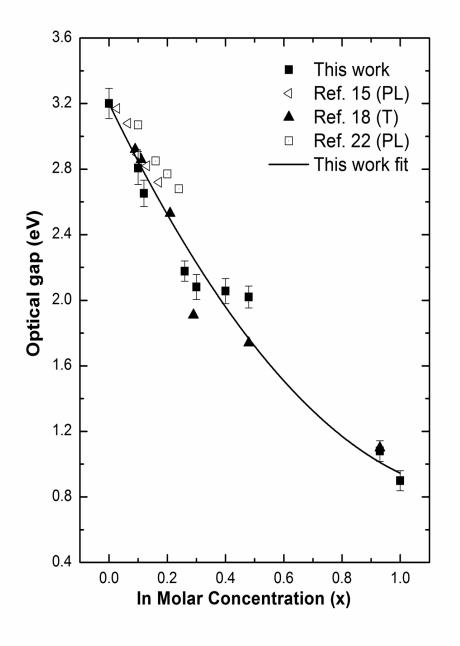**Table 1** Optical parameters from the dielectric function model.
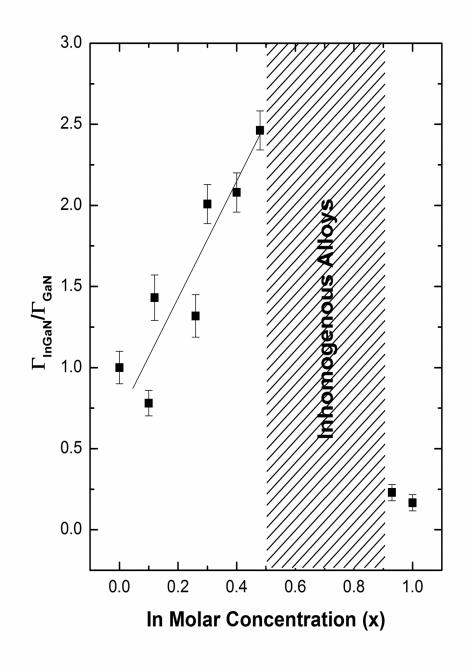
13

Figure 1

Figure 2

Figure 3

Figure 4

17

Figure 5

Table 1

	n_∞	ω_g (eV)	f_j	ω_j (eV)	Γ_j (eV)	Layer Thickness (nm)	Cubic phase (%)	Surface Layer Thickness (nm)	AFM RMS Roughness (nm)	χ^2
GaN	2.054	3.21	0.189	3.656	0.931	430 ± 2	99	6.2	1.0	1.3
x =	2.150	2.81	0.225	3.177	0.727	188 ± 2	99	6.5	4.7	1.2
x =	2.130	2.65	0.359	3.398	1.133	185 ± 3	99	5.3	6.9	1.8
x =	2.176	2.18	0.756	3.361	1.228	165 ± 3	96	9.4	7.3	2.7
x =	2.163	2.08	0.852	3.174	1.870	150 ± 3	90	7.9	7.1	2.8
x =	2.141	2.06	0.889	3.139	1.937	130 ± 3	85	8.3	10.3	2.7
x =	2.139	2.02	0.532	3.126	2.930	165 ± 3	85	10.5	12.6	3.3
x =	1.546	1.08	0.338	1.331	0.213	155 ± 2	96	5.7	5.2	2.1
x =	2.606	0.89	0.723	0.916	0.155	230 ± 2	97	5.0	2.8	1.9

Highlights

- Cubic $In_XGa_{1-X}N$ thin films were grown on GaN/MgO by plasma assisted MBE.
- The $In_XGa_{1-X}N$ complex refraction index from 0.6 to 4.75 eV is reported.
- The dispersion relations for several x are obtained by spectroscopic ellipsometry.